Biochemical and Biophysical Research Communications 460 (2015) 831–837

Contents lists available at ScienceDirect

Biochemical and Biophysical Research Communications

journal homepage: www.elsevier.com/locate/ybbrc

ALS-associated P56S-VAPB mutation restrains 3T3-L1 preadipocyte differentiation

Yukako Tokutake [a], Kazunari Gushima [b], Honami Miyazaki [b], Takeshi Shimosato [c], Shinichi Yonekura [a, b, c, *]

[a] Interdisciplinary Graduate School of Science and Technology, Shinshu University, 8304 Minamiminowa, Kamiina, Nagano 399-4598, Japan
[b] Graduate School of Agriculture, Shinshu University, 8304 Minamiminowa, Kamiina, Nagano 399-4598, Japan
[c] Department of Interdisciplinary Genome Sciences and Cell Metabolism, Institute for Biomedical Sciences, Interdisciplinary Cluster for Cutting Edge Research, Shinshu University, 8304 Minamiminowa, Kamiina, Nagano 399-4598, Japan

ARTICLE INFO

Article history:
Received 17 March 2015
Available online 28 March 2015

Keywords:
ALS
Adipocyte
VAPB
Differentiation
UPR

ABSTRACT

Amyotrophic lateral sclerosis (ALS), which is the most common motor neuron disease in adults, is a neurodegenerative disease that involves the selective and systematic death of upper and lower motor neurons. In addition to the motor neuron death, altered metabolic functions, such as dyslipidemia, have also been reported for ALS patients; however, the underlying mechanism remains unknown. In the present study, we investigated the effects of ALS-associated P56S-vesicle-associated membrane protein-associated protein B (VAPB), P56S-VAPB on 3T3-L1 preadipocyte differentiation and on the expression of differentiation-associated genes and unfolded protein response (UPR)-related genes. Experiments with 3T3-L1 cells transfected with wild-type (Wt)-VAPB and P56S-VAPB expression vectors showed that the size of lipid droplets was markedly smaller in P56S-VAPB-expressing cells, although fat accumulated intracellularly. In P56S-VAPB-expressing cells, increased the expression of PPARγ2, aP2, and C/EBPα, the genes deeply involved in adipocyte differentiation, was not observed. Furthermore, the expression levels of the UPR-related ATF4 and CHOP genes were found to be enhanced in the P56S-VAPB-expressing cells. From these results, P56S-VAPB was found to suppress adipocyte differentiation by promoting the activation of the ATF4-CHOP pathway. Given previous reports showing increased ATF4 and CHOP expression levels in neurons of ALS patients, results from the present study suggest that dyslipidemia is caused by enhanced ATF4–CHOP pathway in the adipose tissue of ALS patients.

© 2015 Elsevier Inc. All rights reserved.

1. Introduction

Amyotrophic lateral sclerosis (ALS) is a rapidly progressive neurodegenerative disorder that affects upper and lower motor neurons [1]. Initially, pathological abnormalities in ALS were thought to be restricted to motor neurons, but descriptions of a wider dissemination of effects throughout the body have challenged this classic paradigm. ALS disease seems to be restricted not only to the CNS but also affects whole-body physiology [2]. In particular, energy metabolism is severely altered in patients with ALS, which has notable clinical implications. Patients with ALS are generally lean with a normal or low body-mass index [3–5] and typically lose weight and body fat as disease progresses [6–8]; therefore, energy stores are decreased. Hyperlipidemia has been put forward as an explanation for energy imbalance in ALS. Previous studies have demonstrated that increased blood lipid concentrations and suggested that the lipid metabolism and the nutritional status of ALS patients are important prognostic factors [9,10]. However, the causes of hyperlipidemia are unclear in patients with ALS.

Although most cases of ALS are sporadic, 5–10% of cases occur in families with at least one other affected family member, and some

Abbreviations: ALS, amyotrophic lateral sclerosis; VAPB, vesicle-associated membrane proteinassociated protein B; UPR, unfolded protein response; PPARγ2, peroxisome proliferator-activated receptor γ2; aP2, adipocyte protein 2; C/EBPα, CCAAT/enhancer binding protein α; ATF4, activating transcription factor 4; CHOP, C/EBP homologous protein; XBP1s, X-box binding protein 1 splicing form; EDEM, degradation enhancing α-mannosidase–like protein; ATF6, activating transcription factor 6.

* Corresponding author. Department of Interdisciplinary Genome Sciences and Cell Metabolism, Institute for Biomedical Sciences, Interdisciplinary Cluster for Cutting Edge Research (ICCER), Shinshu University, 8304 Minamiminowa, Kamiina, Nagano 399-4598, Japan. Fax: +81 265 77 1443.
E-mail address: yonekura@shinshu-u.ac.jp (S. Yonekura).

http://dx.doi.org/10.1016/j.bbrc.2015.03.118
0006-291X/© 2015 Elsevier Inc. All rights reserved.

families display a clear Mendelian inheritance of ALS with high penetrance of the disease [11]. A mutation in the gene encoding vesicle-associated membrane protein-associated protein B (VAPB) causes ALS type-8 and some other related forms of motor neuron disease including late onset spinal muscular atrophy [12]. The mutation that causes ALS type-8 involves a proline to serine substitution at position-56 (P56S-VAPB). VAPB protein is ubiquitously expressed and a type II integral membrane protein that mainly locates at the endoplasmic reticulum (ER). It contains an N-terminal domain homologous to the major sperm protein of nematode worms, a central coiled-coil region and a C-terminal transmembrane domain through which it is anchored in the ER membrane; the N-terminus of VAPB projects from the ER into the cytoplasm [13–15]. VAPB has been proposed to act in the regulation of COPI-mediated protein transport within the Golgi apparatus and from the Golgi back to the ER [16]. VAPB has been implicated in a variety of processes including ER stress and the unfolded protein response (UPR), ER to Golgi transport and bouton formation at the neuromuscular junction [17,18]. ER stress is linked to the pathogenesis of ALS [19,20] and several studies implicate P56S-VAPB in abnormal UPR but the mechanisms are unclear.

Here, we report for the first time that P56S-VAPB impairs lipid droplet formation in 3T3-L1 adipocyte. We also found that P56S-VAPB expressing 3T3-L1 cells restrained the mRNA expression of mature adipocyte marker and enhanced the expression levels of the UPR-related ATF4 and CHOP genes. These results indicate that P56S-VAPB suppress adipocyte differentiation by promoting the activation of the ATF4-CHOP pathway. Our results thus may provide a mechanism by which the energy metabolism is severely altered in ALS.

2. Materials and methods

2.1. Reagents

Dulbecco's modified Eagle's medium (DMEM) was purchased from Gibco (Grand Island, NY). Fetal bovine serum (FBS) was a product of Microbiological Associates (Walkersville, MD). Insulin, 3-isobutyl-1-methylxanthine (IBMX), and dexamethasone were purchased from Sigma (Tokyo, Japan). BODIPY® 493/503 was purchased from Invitrogen (Carlsbad, CA). All other compounds were from Wako Pure Chemical company (Osaka, Japan).

2.2. Plasmids

Human cDNAs encoding VAPB (GenBankTM accession number NM_004738) was amplified using a modification of the method of Kanekura et al. [13]. In briefly, full length cDNA of VAPB was amplified from a human postcentral gyrus cDNA library (Biochain, Hayward, CA) by PCR with a sense primer (5-CGGGATCCACCAATGG CGAAGGTGGAGCAGGTC-3) and an antisense primer (5-GGAAT TCCTACAAGGCAATCTTCCCAATAATTAC-3). P56S-VAPB was obtained by a QuikCahnge Site-Directed mutagenesis kit (Agilent Technologies). Wt-VAPB-GFP and Wt-VAPB-Ds-Red, P56S-VAPB-Ds-Red were produced by cloning into pEGFP-C1 (Clontech) and pDs-Red-monomer-C1 (Clontech), respectively. The sequences of all PCR products were verified by sequencing.

2.3. Cell culture and transfection

Low passage number 3T3-L1 cells were obtained from ATCC (Manassas, VA). 3T3-L1 cells were grown in DMEM containing 10% fetal bovine serum. Cells were transfected using Lipofectamine 2000 (Invitrogen) according to the manufacturer's protocol.

For subcellular localization analysis, 6 h after transfection, cells were washed with phosphate-buffered saline (PBS) and fixed with 4% paraformaldehyde in PBS for 30 min. The cells were observed with Olympus (Tokyo, Japan) FV1000 confocal laser-scanning microscope.

For the induction of adipocyte differentiation, 6 h after transfection, cells were treated with differentiation medium containing 10% fetal bovine serum, 0.5 mM IBMX, 1 μM dexamethasone, and 1.7 μM insulin. Quantitative RT-PCR and BODIPY staining experiments were performed on day 3 or 6 or 10 after initiation of differentiation.

2.4. Oil-red O sating

To quantify lipid accumulation, 3T3-L1 cells were fixed with 10% formalin in PBS for 10 min, rinced with 60% isopropanol, and stained by Oil-red O in 60% isopropanol for 30 min. After the staining, cells were rinsed several times with PBS and subjected to microscopic analysis.

2.5. BODIPY staining and visualization

Adipocytes are visualized by staining lipid droplets with the fluorescent dye, BODIPY 493/503. A fresh solution of BODIPY 493/503 diluted in PBST (PBS supplemented with 0.1% Tween-20) was used for staining. For fixative staining, 3T3-L1 cells were incubated in 4% paraformaldehyde solution for 15 min. After paraformaldehyde solution was removed, the cells were incubated in a volume of 500 μL of 1 μg/mL BODIPY 493/503 for 1 h at room temperature. Images were collected with an Olympus FV1000 confocal laser-scanning microscope. The diameter of lipid droplets in each image was measured with ImageJ software program. With this method, we measured 300 cells in each group.

2.6. Quantitative RT- PCR

Total RNA was isolated from 3T3-L1 cells using the TRIzol reagent (Life Technologies), according to the manufacturer's instructions. The concentration of the isolated total RNA was determined by measuring the optical density at 260 nm, and the purity of the RNA was determined based on the ratio of the absorbance at 260 nm relative to the absorbance at 280 nm. Samples were then processed for cDNA synthesis using a ReverTra Ace® qPCR RT Master Mix with gDNA Remover (TOYOBO, Japan). Real-time PCR was carried out in a 20-μL reaction mixture containing 50 ng cDNA, 0.4 μM each primer, 10 μL SYBR® Premix Ex TaqTM II (TaKaRa Biotechnology, Japan). The primer sequences are shown in Table 1 β-actin was used as an endogenous controls. All the quantitative RT-PCRs were performed in triplicate on Thermal Cycler Dice® Real Time System (TaKaRa), based on a standard curve method. The sensitivity of the reaction and amplification of contaminating products such as the extension of self-annealed primers were evaluated by amplifying serial dilutions of cDNA. All data analysis was performed as recommended by the manufacturer.

2.7. Statistical analysis

In all experiments, values are expressed as means ± standard error of the mean, with at least 3 repeats in each experimental group. Statistical significance was estimated by Student's *t*-test. The test was considered significant at $P < 0.05$.

Table 1
Sequences of primers used for real-time PCR amplification.

Gene	Primers (5′ to 3′)	
PPARγ	Forward	GATGCACTGCCTATGAGCACTT
	Reverse	AGAGGTCCACAGAGCTGATTCC
C/EBPα	Forward	TGAGCCGTGAACTGGACACG
	Reverse	CAGCCTAGAGATCCAGCGAC
aP2	Forward	CACCGCAGACGACAGGAAG
	Reverse	GCACCTGCACCAGGGC
ATF4	Forward	GAGCTTCCTGAACAGCGAAGTG
	Reverse	TGGCCACCTCCAGATAGTCATC
CHOP	Forward	CCTAGCTTGGCTGACAGAGG
	Reverse	CTGCTCCTTCTCCTTCATGC
XBP1s	Forward	TGAGAACCAGGAGTTAAGAACACG
	Reverse	CCTGCACCTGCTGCGGAC
EDEM	Forward	GGATCCCCTATCCCTCGGGT
	Reverse	GTTGCTCCCGCAAGTTCCAG
ATF6	Forward	CTTCCTCCAGTTGCTCCATC
	Reverse	CAACTCCTCAGGAACGTGCT
β-actin	Forward	CTGGGACGACATGGAGAAGA
	Reverse	AGAGGCATACAGGGACAGCA

3. Results and discussion

3.1. P56S mutation leads to aberrant aggregation of VAPB in 3T3-L1 cells

Studies with the motor neuron cell line NSC34 have shown that P56S-VAPB cytosolic aggregates [13,21]. We observed their subcellular distribution using the murine adipocyte cell line 3T3-L1 transfected with the Wt-VAPB and P56S-VAPB expression vectors containing Ds-Red at the C-terminus. The result demonstrated aggregation of P56S-VAPB in 3T3-L1 cells, similar to as observed in NSC34 cells (Fig. 1A). We also observed their subcellular distribution in 3T3-L1 cells co-transfected with GFP-tagged Wt-VAPB and Ds-Red-tagged P56S-VAPB, and found that Wt-VAPB co-localizes with P56S-VAPB (Fig. 1B). This result is consistent with results from previous studies using NSC34 cells [13,14], suggesting that P56S-VAPB recruits Wt-VAPB, thereby inhibiting Wt-VAPB function. Next, we evaluated the adipocyte differentiation potential of Wt-VAPB-expressing and P56S-VAPB-expressing 3T3-L1 cells by oil red O staining. Ds-Red-expressing 3T3-L1 cells were used as a control. The results revealed that the size of lipid droplets was smaller in P56S-VAPB expressing cells while intracellular fat accumulation occurred (Fig. 1C).

3.2. P56S mutation impairs the lipid droplet formation in differentiating 3T3-L1 cells

To study the size of lipid droplets in P56S-VAPB-expressing cells in more detail, lipid droplets in Ds-Red-, Wt-VAPB-, and P56S-VAPB-expressing cells in the differentiation process were stained with BODIPY 493/503 and were observed under a microscope. And then, we measured lipid droplet areas based on images of the cells. On day 3 after induction, no appreciable differences among transfected cells were found in the lipid droplet area per cell (Fig. 2). On day 6 after induction, while lipid droplet areas in Ds-Red- and Wt-VAPB-expressing cells increased, the lipid droplet area in P56S-VAPB-expressing cells was significantly smaller than that of the other transfectants and its size remained unchanged from day 3 onwards (Fig. 2). On day 10 after induction, differentiation was further induced, and the differences were more prominent. In other words, the size of lipid droplets in P56S-VAPB-expressing cells was found to have stayed constant since day 3 of differentiation-stimulating induction.

3.3. P56S mutation restrains the expression levels of differentiated-associated genes in differentiating 3T3-L1 cells

Next, we analyzed the expression levels of differentiation-associated genes over the course of differentiation in Ds-Red-, Wt-VAPB-, and P56S-VAPB-expressing cells using qRT-PCR. Although the expression levels of the PPARγ2 gene in Ds-Red- and Wt-VAPB-expressing cells increased with differentiation, no such increase was observed in P56S-VAPB-expressing cells (Fig. 3). Similar to the PPARγ2 gene expression levels, expression levels of aP2 and C/EBPα genes also increased with the progression of differentiation in Ds-Red- and Wt-VAPB-expressing cells, but not in P56S-VAPB-expressing cells (Fig. 3). The terminal differentiation of preadipocytes into adipocytes has been shown to be initiated by the activation of the transcription factors C/EBPα and PPARγ2 in preadipocytes [22,23]. The expression of these transcription factors involved in adipocyte differentiation was found to be suppressed in P56S-VAPB-expressing cells. It has been known that the aP2 gene expression level is regulated by PPARγ2 [23], and that the aP2 protein affects insulin sensitivity and lipid metabolism [24]. aP2 is involved in the induction of triglyceride (TG) synthase [25] and has also been reported to be involved in cellular uptake of fatty acids [26]. Therefore, it is conceivable that P56S-VAPB suppresses aP2 gene expression and reduces cellular uptake of fatty acids. Thus, it is predicted that this is a cause of hyperlipidemia in ALS patients.

3.4. P56S mutation enhances the expression levels of ATF4 and CHOP in 3T3-L1 cells

Further, the expression levels of UPR-related genes during the differentiation process were measured for Ds-Red-, Wt-VAPB-, and P56S-VAPB-expressing cells using qRT-PCR. The result showed no significant differences in expression levels of XBP1s, EDEM, and ATF6 genes among these cells (Fig. 4). When IRE1 is activated, spliceosome-independent frame switch splicing is induced, and the active form of the transcription factor XBP1s is produced from the spliced substrate XBP1 mRNA [27]. In recent years, XBP1s has been reported to be involved not only in UPR-associated transcription induction but also in the regulation of the expression of PPAR-γ2 and C/EBPα in adipocytes [28]. Moreover, P56S-VAPB has been reported to inhibit the IRE1−XBP1 pathway in studies using NSC34 cells [13], but this effect was not observed in the present study using 3T3-L1 cells. Although additional studies are necessary, this difference suggests that the effect of P56S-VAPB on the IRE1-XBP1 pathway may vary depending on the cell type. Meanwhile, the expression levels of ATF4 and CHOP genes measured at 3 days after differentiation-inducing stimulation were found to be significantly higher in P56S-VAPB-expressing cells than in Ds-Red- or Wt-VAPB-expressing cells (Fig. 4). CHOP is a member of the C/EBP family, and its expression is induced by ATF4 [29]. It contains a leucine zipper structure at the C-terminus and is capable of binding to other C/EBP family members. However, because its DNA binding domain contains two proline residues, CHOP homodimerizes or heterodimerizes, and other C/EBP members cannot bind to the C/EBP-binding sequence [30]. Based on this characteristic structure, CHOP is presumed to serve as an endogenous dominant-negative form to inhibit the functions of other C/EBP members, and it has been reported that forced expression of CHOP indeed results in the suppression of the differentiation of 3T3-L1 cells into adipocytes [31]. In addition, *ATF*-knockout mice have also been shown to be skinny [32]. Moreover, expression of ATF4 and CHOP genes has been reported to be enhanced in corticospinal motor neurons and spinal motor neurons of the transgenic mice expressing P56S-VAPB in a neuron-specific manner [33]. Although the detailed mechanism has not been elucidated, VAPB is believed to be a molecule

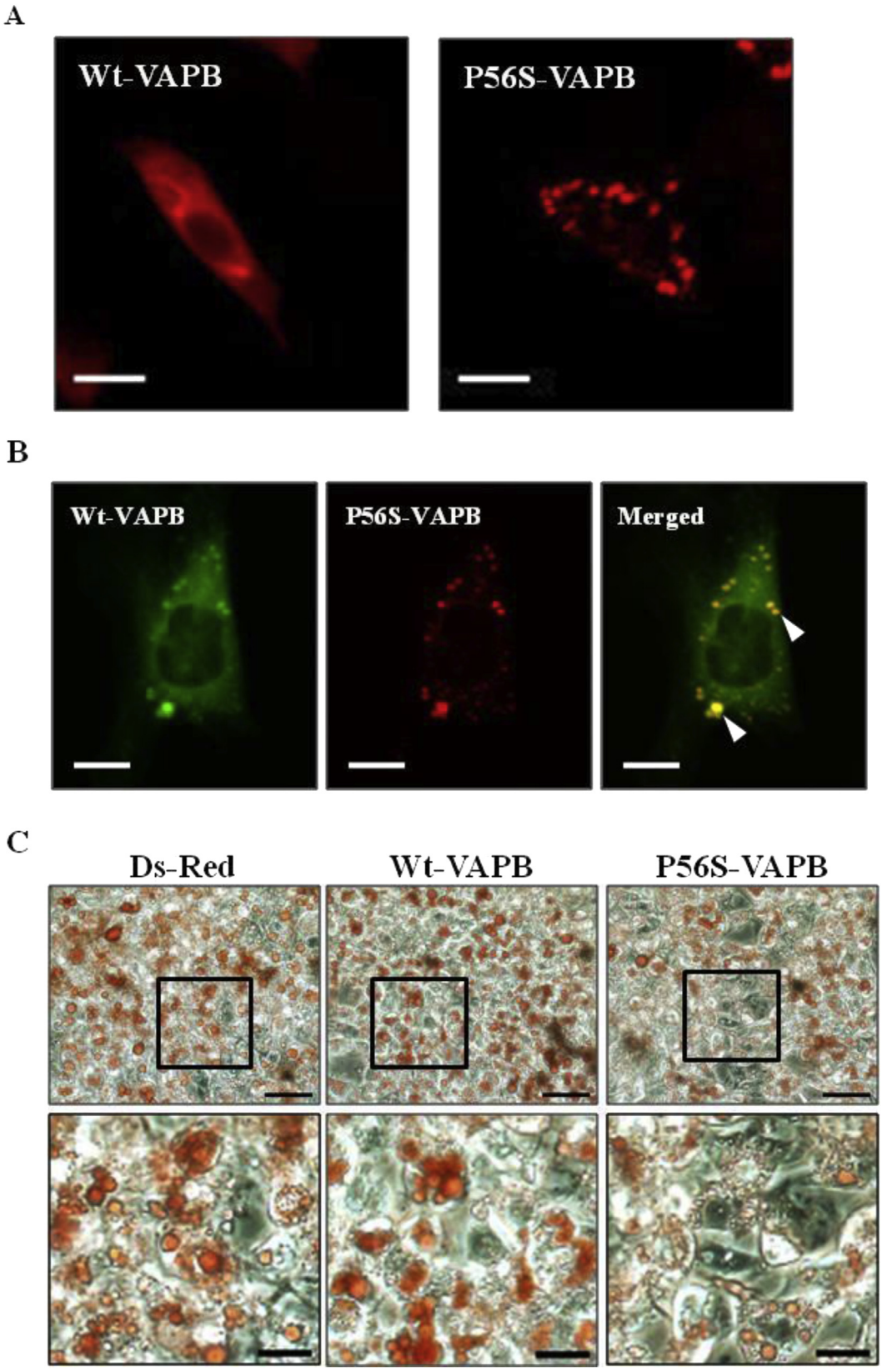

Fig. 1. P56S mutation leads to aberrant aggregation of VAPB in 3T3-L1 cells. A: 3T3-L1 cells were transfected with the indicated plasmids and fixed 48 h after transfection. The distribution of VAPB protein is indicated by Ds-Red. B: 3T3-L1 cells were cotransfected with the vectors encoding C-terminally GFP-fused Wt-VAPB and Ds-Red-fused P56S-VAPB and fixed 48 h after transfection. Scale bar = 20 μm. A merge show on the right. Examples of co-localization are indicated with arrowheads. C: 3T3-L1 cells were transfected with the indicated plasmids and cells were treated with differentiation medium 6 h after transfection. On day 10 after initiation of differentiation, cells were stained with Oil-red O. Low- (*upper*: bar = 50 μm) and high-magnification (*lower*: bar = 20 μm) of Oil-red O staining. This is representative of three similar experiments.

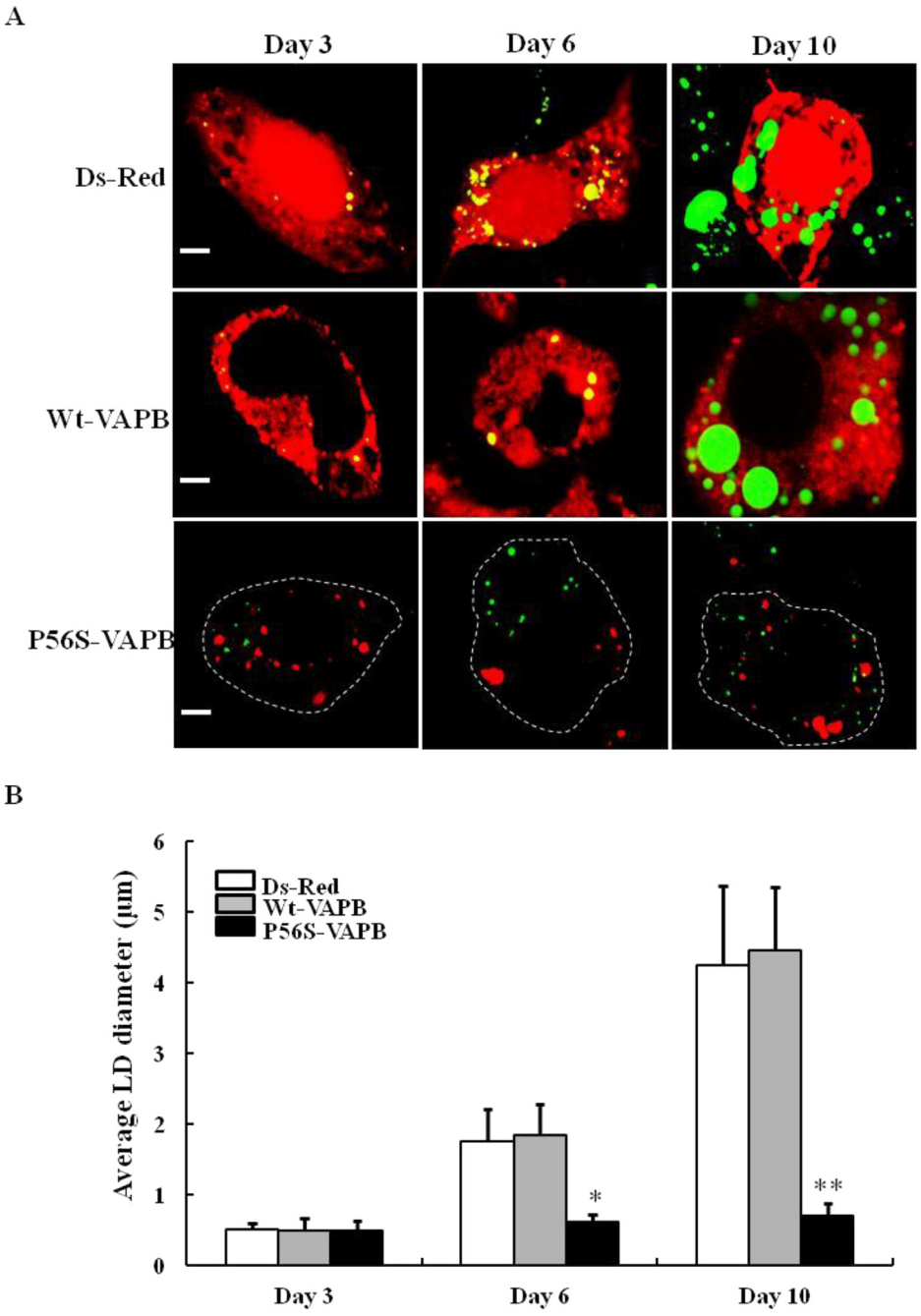

Fig. 2. P56S mutation impairs the lipid droplet formation in differentiating 3T3-L1 cells. A: 3T3-L1 cells were transfected with the vectors encoding Ds-Red or C-terminally Ds-Red-fused Wt-VAPB or Ds-Red-fused P56S-VAPB. For the induction of adipocyte differentiation, 6 h after transfection, cells were treated with differentiation medium. On day 3 or 6 or 10 after initiation of differentiation, adipocytes were visualized by staining lipid droplets with the fluorescent dye, BODIPY 493/503 (green). Images were collected with an Olympus FV1000 confocal laser-scanning microscope. The dotted lines delineate the single adipocyte. Scale bar = 5 μm. B: To quantify the size of lipid droplets, the diameter of lipid droplets in each image was measured with ImageJ software program. The values are the means ± standard deviation for 300 cells in each groups. $^{*}P < 0.05$, $^{**}P < 0.01$ compared with Ds-Red. (For interpretation of the references to color in this figure legend, the reader is referred to the web version of this article.)

that is located in the endoplasmic reticulum and involved in UPR. These findings suggest that P56S-VAPB promoted the ATF4–CHOP pathway activation, thereby suppressing adipocyte differentiation.

About 20% of familial ALS cases are thought to be attributable to SOD mutation. CHOP gene expression has also been shown to be enhanced in the spinal cords of mutant SOD transgenic mice [34] and of sporadic ALS patients [35]. The present study demonstrated that P56S-VAPB enhanced expression of ATF4 and CHOP genes in adipocytes, and it is conceivable that the expression of these genes is also promoted in adipose tissue of patients with other forms of familial ALS or sporadic ALS.

As a result of our investigation on the effects of P56S-VAPB on adipocyte differentiation and the expression of differentiation-associated genes and UPR-related gene using 3T3-L1 cells, we have found that P56S-VAPB suppresses adipocyte differentiation through the promotion of the ATF4–CHOP pathway. In the future, ATF4–CHOP pathway-focused studies with adipose tissues from patients with SOD mutation or sporadic ALS are expected to lead to

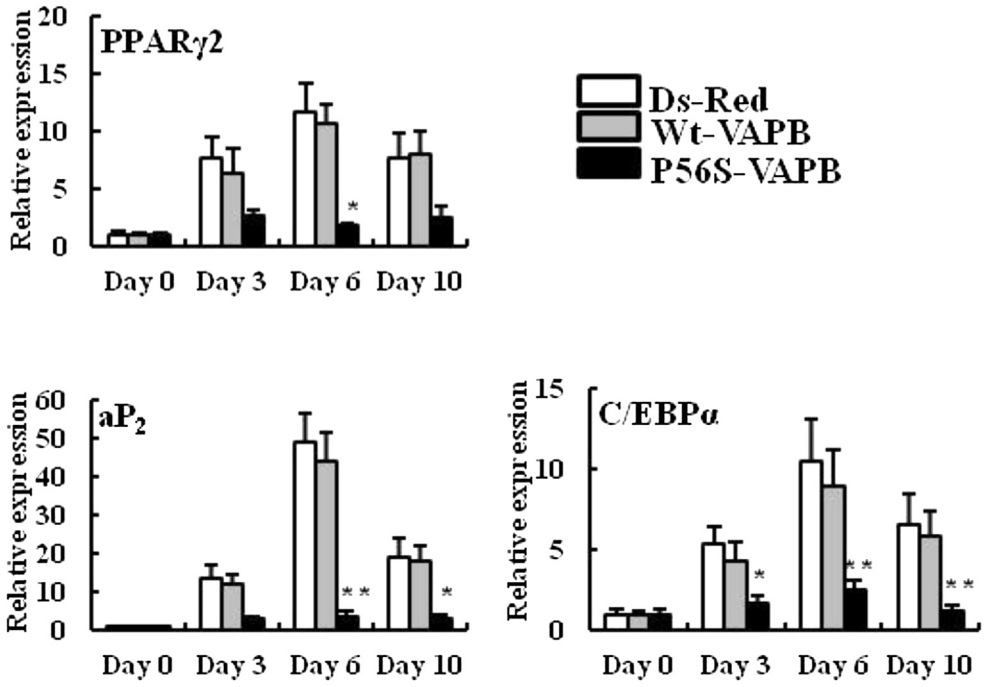

Fig. 3. P56S mutation restrains the expression levels of differentiated-associated genes in 3T3-L1 cells. The mRNA expression of PPARγ2, C/EBPα and aP2 in Ds-Red- or Wt-VAPB- or P56S-VAPB- expressing cells during differentiation induction. The level of mRNA was determined by real-time PCR and normalized by β-actin. The results are expressed as means ± SEM for three independent determinations. $^{*}P < 0.05$, $^{**}P < 0.01$ compared with Ds-Red.

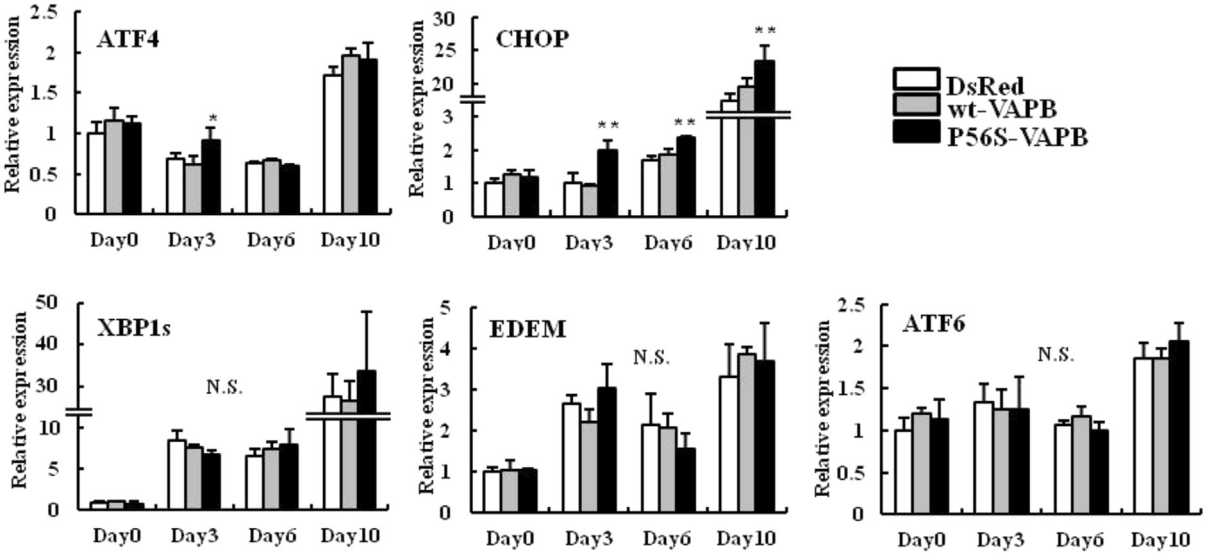

Fig. 4. P56S mutation enhances the expression levels of ATF4 and CHOP in 3T3-L1 cells. The mRNA expression of ATF4, CHOP, XBP1s, EDEM and ATF6 in Ds-Red- or Wt-VAPB- or P56S-VAPB- expressing cells during differentiation induction. The level of mRNA was determined by real-time PCR and normalized by β-actin. The results are expressed as means ± SEM for three independent determinations. $^{*}P < 0.05$, $^{**}P < 0.01$ compared with Ds-Red.

the full understanding of the etiology of dyslipidemia in ALS patients.

Conflict of interest

The authors declare that there are no conflicts of interest.

Acknowledgments

This study was supported in part by “Integration research for agriculture and interdisciplinary fields” (No. 14538629) to Dr. S. Yonekura.

Transparency document

Transparency document related to this article can be found online at http://dx.doi.org/10.1016/j.bbrc.2015.03.118.

References

[1] B.R. Brooks, M. Sanjak, D. Belden, K. Juhasz-Pocsine, A. Waclawik, Natural history of amyotorophic lateral sclerosis, in: R.H. Brown Jr., V. Meininger, M. Swash (Eds.), Amyotorophic Lateral Sclerosis, Dunitz, London, 2000, pp. 31–58.

[2] L. Dupuis, P.F. Pradat, A.C. Ludolph, J.P. Loeffler, Energy metabolism in amyotrophic lateral sclerosis, Lancet Neurol. 10 (2011) 75–82.

[3] N. Vaisman, M. Lusaus, B. Nefussy, E. Niv, D. Comaneshter, R. Hallack, V.E. Drory, Do patients with amyotrophic lateral sclerosis (ALS) have increased energy needs? J. Neurol. Sci. 279 (2009) 26–29.
[4] L. Lacomblez, G. Bensimon, P.N. Leigh, P. Guillet, V. Meininger, Dose-ranging study of riluzole in amyotrophic lateral sclerosis. Amyotrophic lateral sclerosis/riluzole study group II, Lancet 347 (1996) 1425–1431.
[5] J.C. Desport, P.M. Preux, T.C. Truong, J.M. Vallat, D. Sautereau, P. Couratier, Nutritional status is a prognostic factor for survival in ALS patients, Neurology 53 (1999) 1059–1063.
[6] J.C. Desport, P.M. Preux, C.T. Truong, L. Courat, J.M. Vallat, P. Couratier, Nutritional assessment and survival in ALS patients, Amyotroph. Lateral Scler. Other Mot. Neuron Disord. 1 (2000) 91–96.
[7] L.C. Wijesekera, P.N. Leigh, Amyotrophic lateral sclerosis, Orphanet J. Rare Dis. 4 (2009) 3.
[8] E.J. Kasarskis, S. Berryman, J.G. Vanderleest, A.R. Schneider, C.J. McClain, Nutritional status of patients with amyotrophic lateral sclerosis: relation to the proximity of death, Am. J. Clin. Nutr. 63 (1996) 130–137.
[9] L. Dupuis, P. Corcia, A. Fergani, J.L. Gonzalez De Aguilar, D. Bonnefont-Rousselot, R. Bittar, D. Seilhean, J.J. Hauw, L. Lacomblez, J.P. Loeffler, V. Meininger, Dyslipidemia is a protective factor in amyotrophic lateral sclerosis, Neurology 70 (2008) 1004–1009.
[10] J. Dorst, P. Kuhnlein, C. Hendrich, J. Kassubek, A.D. Sperfeld, A.C. Ludolph, Patients with elevated triglyceride and cholesterol serum levels have a prolonged survival in amyotrophic lateral sclerosis, J. Neurol. 258 (2011) 613–617.
[11] L.I. Bruijn, T.M. Miller, D.W. Cleveland, Unraveling the mechanisms involved in motor neuron degeneration in ALS, Annu Rev. Neurosci. 27 (2004) 723–749.
[12] A.L. Nishimura, M. Mitne-Neto, H.C. Silva, A. Richieri-Costa, S. Middleton, D. Cascio, F. Kok, J.R. Oliveira, T. Gillingwater, J. Webb, P. Skehel, M. Zatz, A mutation in the vesicle-trafficking protein VAPB causes late-onset spinal muscular atrophy and amyotrophic lateral sclerosis, Am. J. Hum. Genet. 75 (2004) 822–831.
[13] K. Kanekura, I. Nishimoto, S. Aiso, M. Matsuoka, Characterization of amyotrophic lateral sclerosis-linked P56S mutation of vesicle-associated membrane protein-associated protein B (VAPB/ALS8), J. Biol. Chem. 281 (2006) 30223–30233.
[14] E. Teuling, S. Ahmed, E. Haasdijk, J. Demmers, M.O. Steinmetz, A. Akhmanova, D. Jaarsma, C.C. Hoogenraad, Motor neuron disease-associated mutant vesicle-associated membrane protein-associated protein (VAP) B recruits wild-type VAPs into endoplasmic reticulum-derived tubular aggregates, J. Neurosci. 27 (2007) 9801–9815.
[15] E. Fasana, M. Fossati, A. Ruggiano, S. Brambillasca, C.C. Hoogenraad, F. Navone, M. Francolini, N. Borgese, A VAPB mutant linked to amyotrophic lateral sclerosis generates a novel form of organized smooth endoplasmic reticulum, FASEB J. 24 (2010) 1419–1430.
[16] C.J. Loewen, T.P. Levine, A highly conserved binding site in vesicle-associated membrane protein-associated protein (VAP) for the FFAT motif of lipid-binding proteins, J. Biol. Chem. 280 (2005) 14097–14104.
[17] D.C. Prosser, D. Tran, P.Y. Gougeon, C. Verly, J.K. Ngsee, FFAT rescues VAPA-mediated inhibition of ER-to-Golgi transport and VAPB-mediated ER aggregation, J. Cell. Sci. 121 (2008) 3052–3061.
[18] D. Peretti, N. Dahan, E. Shimoni, K. Hirschberg, S. Lev, Coordinated lipid transfer between the endoplasmic reticulum and the golgi complex requires the VAP proteins and is essential for golgi-mediated transport, Mol. Biol. Cell. 19 (2008) 3871–3884.
[19] S. Saxena, E. Cabuy, P. Caroni, A role for motoneuron subtype-selective ER stress in disease manifestations of FALS mice, Nat. Neurosci. 12 (2009) 627–636.
[20] K. Kanekura, H. Suzuki, S. Aiso, M. Matsuoka, ER stress and unfolded protein response in amyotrophic lateral sclerosis, Mol. Neurobiol. 39 (2009) 81–89.
[21] K. Langou, A. Moumen, C. Pellegrino, J. Aebischer, I. Medina, P. Aebischer, C. Raoul, AAV-mediated expression of wild-type and ALS-linked mutant VAPB selectively triggers death of motoneurons through a Ca^{2+}-dependent ER-associated pathway, J. Neurochem. 114 (2010) 795–809.
[22] Z. Cao, R.M. Umek, S.L. McKnight, Regulated expression of three C/EBP isoforms during adipose conversion of 3T3-L1 cells, Genes. Dev. 5 (1991) 1538–1552.
[23] P. Tontonoz, E. Hu, B.M. Spiegelman, Stimulation of adipogenesis in fibroblasts by PPAR gamma 2, a lipid-activated transcription factor, Cell 79 (1994) 1147–1156.
[24] J.B. Boord, S. Fazio, M.F. Linton, Cytoplasmic fatty acid-binding proteins: emerging roles in metabolism and atherosclerosis, Curr. Opin. Lipidol. 13 (2002) 141–147.
[25] B.M. Spiegelman, M. Frank, H. Green, Molecular cloning of mRNA from 3T3 adipocytes. Regulation of mRNA content for glycerophosphate dehydrogenase and other differentiation-dependent proteins during adipocyte development, J. Biol. Chem. 258 (1983) 10083–10089.
[26] D.W. Waggoner, D.A. Bernlohr, In situ labeling of the adipocyte lipid binding protein with 3-[125I]iodo-4-azido-N-hexadecylsalicylamide. Evidence for a role of fatty acid binding proteins in lipid uptake, J. Biol. Chem. 265 (1990) 11417–11420.
[27] H. Yoshida, T. Matsui, N. Hosokawa, R.J. Kaufman, K. Nagata, K. Mori, A time-dependent phase shift in the mammalian unfolded protein response, Dev. Cell. 4 (2003) 265–271.
[28] H. Sha, Y. He, H. Chen, C. Wang, A. Zenno, H. Shi, X. Yang, X. Zhang, L. Qi, The IRE1alpha-XBP1 pathway of the unfolded protein response is required for adipogenesis, Cell. Metab. 9 (2009) 556–564.
[29] Y. Ma, J.W. Brewer, J.A. Diehl, L.M. Hendershot, Two distinct stress signaling pathways converge upon the CHOP promoter during the mammalian unfolded protein response, J. Mol. Biol. 318 (2002) 1351–1365.
[30] D. Ron, J.F. Habener, CHOP, a novel developmentally regulated nuclear protein that dimerizes with transcription factors C/EBP and LAP and functions as a dominant-negative inhibitor of gene transcription, Genes. Dev. 6 (1992) 439–453.
[31] N. Batchvarova, X.Z. Wang, D. Ron, Inhibition of adipogenesis by the stress-induced protein CHOP (Gadd153), EMBO J. 14 (1995) 4654–4661.
[32] C. Wang, Z. Huang, Y. Du, Y. Cheng, S. Chen, F. Guo, ATF4 regulates lipid metabolism and thermogenesis, Cell. Res. 20 (2010) 174–184.
[33] L. Aliaga, C. Lai, J. Yu, N. Chub, H. Shim, L. Sun, C. Xie, W.J. Yang, X. Lin, M.J. O'Donovan, H. Cai, Amyotrophic lateral sclerosis-related VAPB P56S mutation differentially affects the function and survival of corticospinal and spinal motor neurons, Hum. Mol. Genet. 22 (2013) 4293–4305.
[34] A.S. Vlug, E. Teuling, E.D. Haasdijk, P. French, C.C. Hoogenraad, D. Jaarsma, ATF3 expression precedes death of spinal motoneurons in amyotrophic lateral sclerosis-SOD1 transgenic mice and correlates with c-Jun phosphorylation, CHOP expression, somato-dendritic ubiquitination and golgi fragmentation, Eur. J. Neurosci. 22 (2005) 1881–1894.
[35] J.D. Atkin, M.A. Farg, A.K. Walker, C. McLean, D. Tomas, M.K. Horne, Endoplasmic reticulum stress and induction of the unfolded protein response in human sporadic amyotrophic lateral sclerosis, Neurobiol. Dis. 30 (2008) 400–407.